Thouless and critical regimes in insulating icosahedral AlPdRe ribbons

2003 J. Phys.: Condens. Matter 15 8753

(http://iopscience.iop.org/0953-8984/15/50/009)

INSTITUTE OF PHYSICS PUBLISHING JOURNAL OF PHYSICS: CONDENSED MATTER

J. Phys.: Condens. Matter **15** (2003) 8753–8766 PII: S0953-8984(03)67620-4

Thouless and critical regimes in insulating icosahedral AlPdRe ribbons

J Delahaye, C Berger[1] **and G Fourcaudot**

LEPES-CNRS, Avenue des Martyrs, BP 166, 38042 Grenoble Cedex 9, France

Received 12 August 2003
Published 3 December 2003
Online at stacks.iop.org/JPhysCM/15/8753

Abstract

We present conductivity measurements of quasicrystalline AlPdRe ribbons in a wide range of temperature (20 mK–300 K), for icosahedral samples spanning a broad resistivity range ($R = \rho_{4\,\mathrm{K}}/\rho_{300\,\mathrm{K}}$ from 2 to 209). We focus here on a detailed analysis of the temperature dependence of the conductivity $\sigma(T)$ for the insulating samples ($R > 16$). Three successive regimes are revealed as the temperature is increased to 300 K: a low temperature variable range hopping-like behaviour, followed by a Thouless regime and a high temperature critical regime. The temperature dependence of the inelastic scattering time found elsewhere by magnetoresistance data analysis accounts well for the change of curvature in $\sigma(T)$ and the trends observed as R varies. The present results point to a similar behaviour between quasicrystalline AlPdRe samples and disordered systems close to the metal–insulator transition, in accordance with our previous analysis of the very low temperature insulating regime and of the finding of conductivity scaling laws.

1. Introduction

The icosahedral (i-) alloy Al–Pd–Re is the most resistive quasicrystalline material discovered. Signature of an insulating behaviour has been reported in the most resistive samples [1–5], which was unexpected for an ordered alloy composed of metallic elements. In fact such samples display a strong decrease of the conductivity when the temperature is reduced and the conductivity value σ can fall below 1 $(\Omega\,\mathrm{cm})^{-1}$ at 4 K. Although its microscopic origin is still debated for this class of materials, the metal–insulator (MI) transition has been described by many authors [3, 6–9] in a variety of differently prepared samples.

For samples of increasing resistivity, different regimes were observed. They usually are analysed within the same framework as disordered systems approaching and crossing a MI transition. For less resistive samples, weak localization combined with electron–electron interaction effects accounts well for the conductivity dependence versus magnetic field and temperature. For more resistive samples, weak localization effects break down and an insulating regime is observed. However, regimes in the intermediate temperature range and

[1] Present address: GATECH, School of Physics, Atlanta, GA 30332-0430, USA.

0953-8984/03/508753+14$30.00

close to the MI transition have seldom been studied, and in particular the critical regime (see below) has only been discussed once [7]. Literature values of the transport parameters and the sample resistive characteristics around the transition and further on the insulating side vary widely. Differences in the sample preparation (melt-spun ribbons [2, 3], thin films [9] or cast ingots [1, 5]) could actually yield various structural or chemical microscopic characteristics. Indeed, it is well known that close to a metal–insulator transition, the low temperature resistivity varies significantly with minute changes of microscopic parameters. Another reason is that it can be misleading to analyse data in a reduced temperature range or for a series of samples in a limited resistivity range.

In this context, it is essential to study samples not only made by the same preparation process but also over a significant resistivity range on both sides of the metal–insulator transition. Only this can provide a systematic way to reveal a convincing pattern in a system with too many unknown characteristics. For quasicrystals, indeed, we do not have the equivalent of a well defined disorder parameter, like for instance the doping concentration in a highly doped disordered semiconductor or the volume fraction of metal to insulator in granular systems, both of which are driving parameters for the MI transition in these systems.

In several previous articles, we have reported on conductivity measurements for similarly prepared i-AlPdRe samples, exploring the two ends of our available resistivity range. The less resistive samples, far into the metallic regime, show the effects of weak localization and its breakdown [10] on the magnetoresistance. For the most resistive samples, well into the insulating regime, we have reported [4] on an insulating-like behaviour for the conductivity for temperatures below 1 K. The transition between the two regimes was analysed [7] for metallic samples by a scaling law of the conductivity. The latter articles [4, 7, 10] reach the same conclusion, namely that the set of curves $\sigma(T, R)$ of i-AlPdRe ribbons are similar to what is observed and predicted for disordered systems close to the Mott–Anderson MI transition. This was realized before [11, 12] in less resistive quasicrystalline alloys, such as i-AlCuFe and i-AlPdMn.

With the present paper, we complete the study of the insulating samples by the analysis of the temperature dependence of their conductivity in a broad temperature range (between 20 mK and 300 K) and for samples over a large conductivity range. The i-AlPdRe melt spun ribbons all have the same nominal composition $Al_{70.5}Pd_{21}Re_{8.5}$ (which is an average composition that may differ slightly from the actual one [13]). As already discussed [4, 7], there is a univocal relation between the resistance and its temperature dependence (the lower σ, the higher R), so that the samples are classified and labelled according to their resistance ratio $R = \rho_{4\ \mathrm{K}}/\rho_{300\ \mathrm{K}}$. For our melt-spun ribbons, R values ranged from $R = 2$ to 209. The ratio $R = 209$ is the highest obtained so far for ribbons and is of the same magnitude as the highest published value ($R = 280$ in i-AlPdRe ingots [14]). The MI transition was located [7] in our set of samples around $R \simeq 16$, and thus we focus here on insulating samples with $R = 17$–209.

General conductivity trends for our samples are described in section 2. The models used for disordered systems, and especially for disordered weak insulators, are then presented in section 3. We show in section 4 that our set of curves $\sigma(T, R)$ can be understood with such models. In particular, the possible roles of critical and Thouless regimes are underlined. The question of a specific quasicrystalline feature is also addressed together with the role of disorder in these highly resistive quasicrystalline alloys.

2. Overview of $\sigma(T)$ as a function of the conductivity ratio R

2.1. Experimental details

The i-AlPdRe samples measured here are ribbons obtained by melt-spinning and of nominal composition $Al_{70.5}Pd_{21}Re_{8.5}$. Post-quenching annealing is performed up to 950–1010 °C (the

Table 1. Parameters of the measured ribbons: resistance ratio $R = \rho_{4\,\mathrm{K}}/\rho_{300\,\mathrm{K}}$; conductivity value σ at 4 and 300 K; temperature range of the measurements ΔT; the T^* temperatures correspond to inflexions in the $\sigma(T)$ dependence (see text for details); α and σ_0 are parameters of a $\sigma_0 + \sigma_1 T^\alpha$ fit performed between 300 K and T_2^* (or ≃20 K when T_2^* is not defined). The uncertainty on σ_0 is around 0.2 $(\Omega\ \mathrm{cm})^{-1}$ and therefore the negative value obtained for the sample $R = 175$ is not significant.

R	$\sigma_{4\,\mathrm{K}}$ $(\Omega\ \mathrm{cm})^{-1}$	$\sigma_{300\,\mathrm{K}}$ $(\Omega\ \mathrm{cm})^{-1}$	ΔT (K)	T_0^* (K)	T_1^* (K)	T_2^* (K)	α	σ_0 $(\Omega\ \mathrm{cm})^{-1}$
2.37	170	403	2.5–300				0.97	167
5.83	53.7	313	2.5–300			50	1.02	58.8
14.1	18.2	257	0.4–300			50	1.09	24.2
16.6	15.0	249	0.4–300			50	1.11	19.6
≃17	14.6	248	0.02–5		0.2			
17.9	13.7	245	0.4–300		<0.4	50	1.13	19.8
21.8	10.8	236	0.4–300		<0.4	40	1.13	15.6
29.3	7.63	224	0.4–300		<0.4	30	1.14	10.6
65.7	2.98	196	0.4–300		1.5	20	1.25	3.7
≃67	2.91	195	0.02–5	0.2	1.5			
81.7	2.32	189	0.4–300		2	10	1.28	2.2
128	1.39	178	0.02–300	0.75			1.51	0.8
150	1.16	174	2.5–300				1.66	1.3
175	0.97	170	2.5–300				1.51	−0.1
≃209	0.79	166	0.02–5	1				

maximum temperature changes the R distribution [13]). Representative ribbons have been characterized chemically and structurally. The chemical composition is homogeneous within the ribbons (fluctuations are of the order of 0.5 at.% for the different chemical elements) and sharp x-ray diffraction peaks reflect a high quality quasicrystalline order [13].

Conductivity measurements were performed in three different cryostats: a home-made cryostat for the range 2.5–300 K; an He_3 cryostat for the range 0.4–10 K; and a dilution cryostat between 20 mK and 5 K. Details of the conductivity set-up measurements can be found in [4, 7].

Since the absolute value of the conductivity can only be roughly estimated in an irregularly shaped sample, it was deduced [13] from an empirical relation between the resistance ratio $R = \rho_{4\,\mathrm{K}}/\rho_{300\,\mathrm{K}}$ (that could be precisely measured) and the conductivity at 300 K. A summary of the sample parameters, temperature range of the measurement and characteristic temperatures used for the analysis (defined below) are summarized in table 1.

2.2. General description of the conductivity $\sigma(T)$

The main features of the conductivity data $\sigma(T, R)$ are presented in figures 1–3. In the following, we will call the *positive (negative) concavity region* the region of the curves where $\mathrm{d}^2\sigma/\mathrm{d}T^2 > 0$ ($\mathrm{d}^2\sigma/\mathrm{d}T^2 < 0$), respectively.

Above ≃100 K, it is clear from figure 1 that all the curves $\sigma(T, R)$ are roughly parallel to each other, independently of their insulating or metallic character. Looking more closely between 300 and 30 K, it appears that the curves evolve from a linear T dependence ($\sigma(T) = \sigma_0 + \sigma_1 T$) for the ribbons of lowest R ($R \simeq$ 2–5), towards a dependence of the form

$$\sigma(T) = \sigma_0 + \sigma_1 T^\alpha \tag{1}$$

for samples of higher R ($\alpha > 1$). The exponent α increases steadily with R up to $\alpha \simeq 3/2$, with even an exponent 1.7 in a ribbon with $R = 150$ (see table 1).

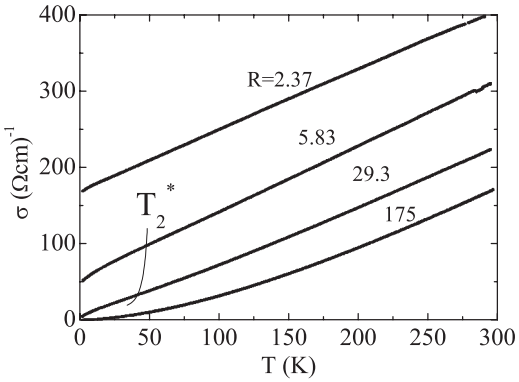

Figure 1. The temperature dependence of the conductivity $\sigma(T, R)$, in the range 2.5–300 K, for ribbons with $R = 2.37$, 5.83, 29.3 and 175 (from top to bottom).

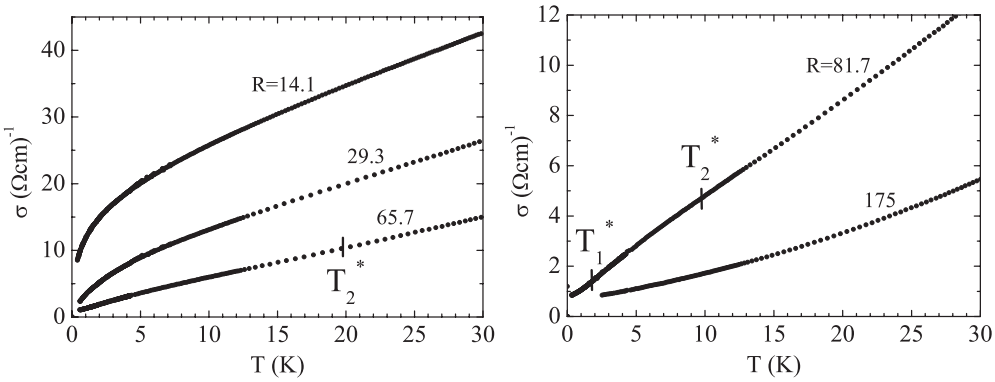

Figure 2. The temperature dependence of the conductivity $\sigma(T, R)$, in the range 0.4 (or 2.5 K)–30 K, for ribbons with $R = 14.1$, 29.3 and 65.7 (left-hand panel) and $R = 81.7$ and 175 (right-hand panel).

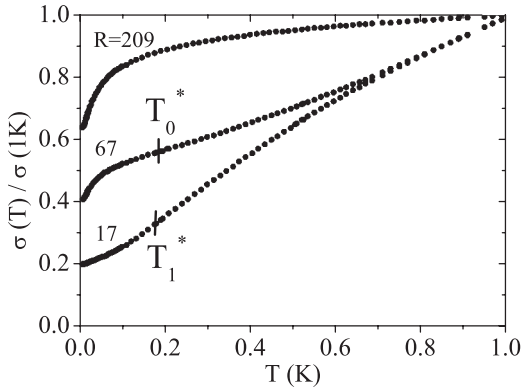

Figure 3. The temperature dependence of the conductivity $\sigma(T, R)$ normalized at 1 K, with T between 20 mK and 1 K, for ribbons $R = 209$, 67 and 17 (from top to bottom).

Between 30 and 1 K (figure 2) and for intermediate resistance ratios ($5 < R < 80$) a concavity change occurs, from positive at high temperature to negative at low temperature.

This concavity change defines a first characteristic temperature, labelled T_2^*. This temperature does not evolve significantly across the MI transition and it goes from 50 K for $R \simeq 5$ down to 10 K for $R \simeq 80$ (see table 1).

Below 1 K (see figure 3) and on the insulating side of the MI transition (i.e. $R > 16$), a plateau appears. By plateau we mean a region with a reduced T dependence for the conductivity and that extrapolates to a finite σ value at zero temperature. This plateau might also be present on the metallic side of the transition but at a much lower temperature, since it was not observed on metallic ribbons down to 400 mK. For the samples where T_2^* is defined, the plateau onset induces another change of concavity from negative to positive when the temperature is lowered. This new inflexion point, which ends the negative concavity region, defines a second characteristic temperature T_1^*. We emphasize that this plateau is not due to thermalization issues, since it appears at as high as 200 mK for a sample of $R \simeq 17$. It was shown in [15] that cooling is efficient in our experiment down to 20 mK. The temperature T_1^* increases with the resistance ratio R from 200 mK at the MI transition ($R = 17$) up to 2 K for the last sample where a negative concavity region could be defined ($R = 81.7$).

This plateau is followed at even lower temperatures by a further decrease of the conductivity, which plummets as T goes to zero. Such a decrease is not visible in the sample with $R = 17$ but it clearly appears for $R = 67$. This new inflexion point, labelled T_0^*, is present in all the insulating ribbons and marks the transition between the plateau and the very low temperature decrease. T_0^* increases with R, with $T_0^* = 200$ mK, 750 mK and 1 K in samples with $R = 67$, 128 and 209 respectively.

A schematic drawing of $\sigma(T)$ curves is presented for ribbons with $R \simeq 60$ and 100 in figure 4. The different transport regimes proposed in the next section are also reported.

3. Models in disordered systems

Theories for disordered systems predict that close to the MI transition, and at finite temperature, the conductivity of a disordered system is determined by the ratio of two lengths: L_T and ξ. L_T is the inelastic scattering length at temperature T and ξ is either the correlation length on the metallic side of the MI transition or the localization length on the insulating side. L_T decreases with increasing temperature, and in general L_T can also depend on parameters such as the presence of magnetic impurities, frequency, etc. We can distinguish three regimes. The critical regime of the MI transition is characterized by $L_T < \xi$, whereas the metallic and insulating regimes correspond to $L_T > \xi$. Physically the metallic and insulating regime can only be discriminated for lengths larger than ξ, where the full electronic pattern has developed. In other words, if $L_T < \xi$ the metallic and insulating regime cannot be distinguished (for the same L_T) [16], and the predicted temperature dependence of conductivity is symmetrical on both sides close to the transition. Note that the following models are valid only for length scales larger than the elastic mean free path L_{el}.

3.1. The metallic side of the MI transition

3.1.1. Metallic regime. For $L_T > \xi$ ($T < T_1$) the conductivity can be written [17, 18]

$$\sigma(T) = \frac{e^2}{\hbar}\left(\frac{A}{\xi} + \frac{B}{L_T}\right) \tag{2}$$

where A and B are two constants close to unity. In this regime, the usual relation $L_T = (D_\infty \tau_T)^{1/2}$ is valid, with D_∞ the diffusion constant at zero temperature and τ_T the inelastic scattering time. The term proportional to $1/\xi$ corresponds to the residual conductivity at zero

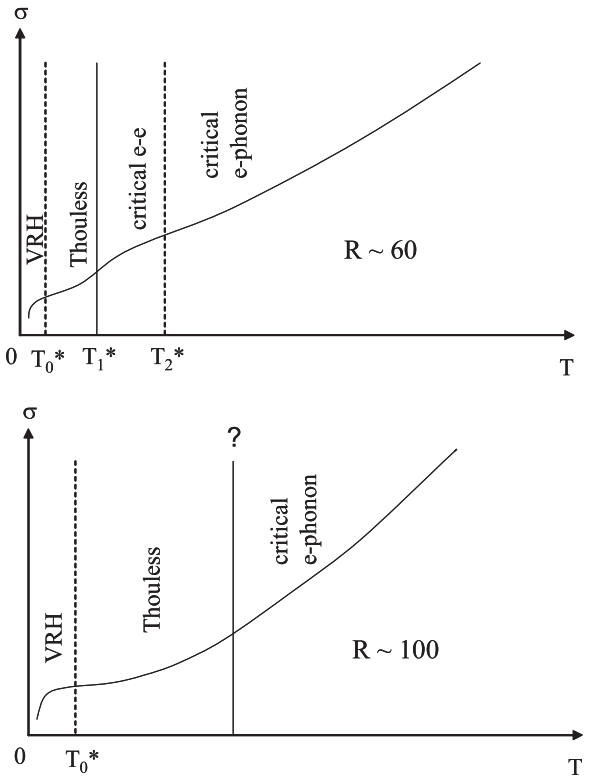

Figure 4. A schematic drawing of the curve $\sigma(T)$ and characteristic temperatures T_2^*, T_1^* and T_0^*. Top panel: a hypothetical ribbon with $R \simeq 60$. Bottom panel: a ribbon with $R \simeq 100$. The temperature range for the different regimes proposed (see the text) is reported.

temperature. According to the scaling theory without interactions [19], ξ goes to infinity when the MI transition is approached, and the residual conductivity goes to zero continuously. The term proportional to $1/L_T$ contains the temperature dependence of the conductivity.

3.1.2. Critical regime. If $L_T < \xi$ ($T > T_1$), equation (2) remains valid but the second term becomes dominant. The effective diffusion coefficient is now temperature dependent, which leads to the relation $L_T = (D_\infty \xi \tau_T)^{1/3}$. The temperature dependent part of the conductivity is finally given by equation [16, 17]

$$\delta\sigma(T) = \frac{Be^2}{(A\hbar^2)^{1/3}} N(E_F)^{1/3} \frac{1}{{\tau_T}^{1/3}}. \tag{3}$$

This regime is also called the microscopic diffusion regime. One important prediction is that if the density of states at the Fermi level is weakly dependent on the disorder parameter n, then the curves $\sigma(T, n)$ are parallel to each other for different values of n.

3.2. The insulating side of the MI transition

If $L_T > \xi$, two regimes are possible: the variable range hopping (VRH) and the Thouless regimes.

3.2.1. Variable range hopping. If $k_B T$ is smaller than the average energy difference between localized states at distance ξ, then transport occurs via VRH [20]. The basic idea is that an electron localized on a region of size the order of the localization length ξ may preferentially hop to localized sites which are close in energy, but not necessarily close spatially. The localization length ξ is disorder dependent, and the smaller ξ, the lower the conductance, the more insulating the sample. More specifically, if the density of states is constant on the energy scale $k_B T$, it can be shown in 3D that [21, 22]

$$\sigma(T) = \sigma_1 \exp[-(T_0/T)^{1/4}]. \tag{4}$$

The Mott temperature T_0 given by $k_B T_0 \simeq 18/[\xi^3 N(E_F)]$ goes to zero at the MI transition.

3.2.2. Thouless regime. In the case where the localization length is large compared with the distance between two localized sites, Thouless has predicted [23, 24] a particular conduction mechanism. On each localization site of size the order of ξ, an electron can diffuse up to the localization length ξ above which diffusion is stopped, by definition of the localization length ξ. But after a characteristic time τ_T (the inelastic scattering time) it can hop to another localized site. The effective diffusion coefficient of this random walk is thus given by $D = \xi^2/\tau_T$. With the Einstein relation, the conductivity follows

$$\sigma(T) \simeq e^2 N(E_F) \xi^2/\tau_T. \tag{5}$$

This regime can in principle be experimentally distinguished from the critical regime because even if $N(E_F)$ does not change with disorder, the curves $\sigma(T, n)$ are not parallel for different n because the pre-factor is ξ (and thus n) dependent. But if a temperature range such as $T > T_0$ and $L_T > \xi$ can in principle always be found close enough to the MI transition, the possibilities to observe the Thouless regime will depend sharply on the system parameters [25]. Indeed, such a regime is only seldom reported in experimental studies of the MI transition of disordered systems.

3.2.3. Critical regime. If $L_T < \xi$, the sample is in the critical regime of the MI transition. As explained above, no discontinuity is expected in this regime for the curves $\sigma(T, n)$ across the MI transition, which are therefore given by equation (3).

3.3. Inelastic mean free path

In order to determine the actual T dependence of σ in the different regimes from the above relations, we have to know the T dependence of τ_T. Generally, τ_T depends on many processes [17], such as electron–electron scattering, electron–phonon scattering, two level system processes, scattering on magnetic impurities, etc. The actual dependence is dominated by the shortest among these characteristic times. The T dependence of τ_T is usually well described by an inverse power law, i.e. $1/\tau_T \propto T^p$, where the exponent p depends on the temperature range and the disorder strength.

Electron–electron scattering usually dominates at low temperature (below $\simeq$30 K). In non-crystalline materials or materials with short mean free path [21]

$$1/\tau_T = CT^2 + DT^{3/2}. \tag{6}$$

The second term, that does not appear in the usual relation of Landau–Baber ($1/\tau_T \propto T^2$), becomes larger when disorder increases. At higher temperatures, the electron–phonon scattering dominates and the p exponent depends on the T range: for $T > \theta_D$ (Debye temperature), $1/\tau_T \propto T$ whereas for $T < \theta_D$, $1/\tau_T \propto T^3$ (weak disorder) or $1/\tau_T \propto T^4$

(strong disorder) [26]. These expressions are established for disordered metals, and it is usually assumed that they are still valid across the transition.

Electron–electron interaction effects when disorder is present yield a square root T dependence of σ at low temperature [27]. This effect can be accounted for by introducing a new length L_{int} in equation (2) instead of L_T,

$$L_{\text{int}} = \sqrt{\frac{\hbar D}{k_B T}}. \tag{7}$$

This length corresponds physically to the interaction time $\tau_{\text{int}} \simeq \hbar / k_B T$.

According to these models we thus expect a variety of shapes for $\sigma(T)$, depending on the dominant inelastic process. Moreover, for a given inelastic process and a given regime, the temperature dependence is predicted to evolve with disorder. A schematic summary is presented in figure 5.

4. Discussion

4.1. Interpretation of the conductivity curves

The relevance of disordered systems theories for metallic i-AlPdRe ribbons has already been emphasized and discussed in previous articles [7, 10]. For ribbons of small R ratio ($R = 2$–5), the temperature and magnetic field dependence of conductivity follow, at least qualitatively, weak localization corrections [10]. For ribbons closer to the MI transition, weak localization theories breakdown since the low T quantum corrections are no longer small. We have shown [7] that very close to the transition the $\sigma(T)$ dependence can still be described by disordered systems models provided that the critical regime is taken into account.

Here, we aim at discussing $\sigma(T, R)$ curves of insulating i-AlPdRe ribbons. We show below that most of the experimental features can be qualitatively explained within the theoretical framework presented above, R playing the role of the disorder parameter n.

At high enough temperature, but still in the range $L_T > L_{\text{el}}$, all the samples are expected to be in the critical regime of the MI transition. This explains that the curves $\sigma(T, R)$ of different Rs are parallel around 300 K (assuming that the density of states is only weakly R dependent across the MI transition). According to equation (3), a power law $\sigma(T) \propto T^{\alpha}$ is expected, with $\alpha = p/3$. For electron–phonon scattering, expected to be dominant above roughly 30 K, p is between 3 and 4, and α is thus between 1 and $4/3$ (the Debye temperature in i-AlPdRe is around 400 K [28]). This agrees well with our observation, except for the most resistive ribbons ($R \simeq 100$) which have slightly higher α values in the range 30–300 K. The slow increase of the exponent α with R may come from a change of p with the resistivity (i.e. the equivalent of the disorder strength) as it is predicted for disordered systems.

For samples close to the MI transition, the localization length is large and the critical regime is expected to be dominant down to very low temperatures. Following figure 5, a critical regime dominated by electron–electron scattering is characterized by an exponent α between $2/3$ and $1/2$ (even $1/3$ at very low temperatures, under electron–electron interaction effects). Experimental findings agree with this picture since a negative concavity region, i.e. a range of temperature with a local exponent α below 1, is observed between T_2^* and T_1^*. Then T_2^* would determine the transition between an electron–electron and an electron–phonon dominated scattering, whereas T_1^* marks the end of the high temperature critical regime and the onset of the Thouless regime (see below). The T_2^* values of table 1 are found between 10 and 50 K, which is consistent with the general consensus for the temperature range where scattering is dominated by electron–phonon effects. Note that for samples of higher R, ξ decreases, and

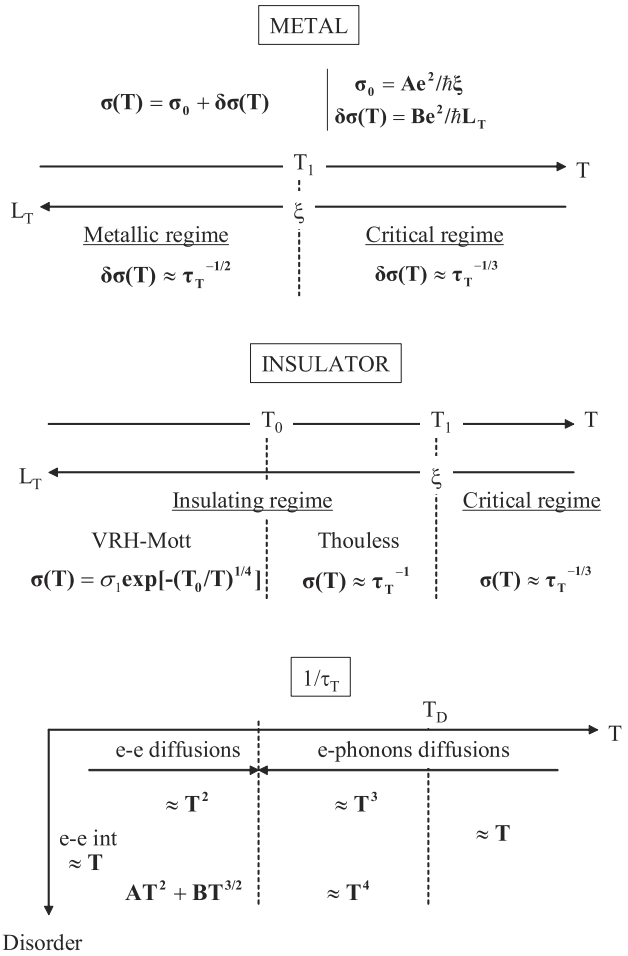

Figure 5. A summary of the relations between σ and τ_T and between $1/\tau_T$ and temperature. Top panel: different regimes expected on the metallic side of the MI transition. Middle panel: different regimes expected on the insulating side. Bottom panel: the temperature dependence of $1/\tau_T$ as a function of temperature and disorder strength.

for a similar L_T, the critical regime is shifted to a higher temperature range, where the dominant scattering mechanism is expected to be electron–phonon type. This naturally explains why, for high enough R, a negative exponent is not observed in the conductivity for this temperature range ($T_1 > T_2^*$).

For samples deeper in the insulating state, the insulating regime is expected to develop more and more clearly at low temperatures. We propose that the positive concavity in the intermediate temperature range above T_0^* corresponding to the plateau (see also figure 5) is due to the Thouless regime. Indeed, a Thouless regime is characterized by power laws with an exponent α between 1 (low temperature electron–electron interaction), and 2 (intermediate temperature electron–electron scattering) or even 3 (higher temperature electron–phonon scattering) depending on the inelastic process considered. For instance, in the case of strong disorder and electron–electron scattering, $\sigma(T) = CT^{3/2} + DT^2$ is predicted in the Thouless regime. This $\sigma(T)$ law fits well the conductivity of a ribbon with $R = 175$, as shown in

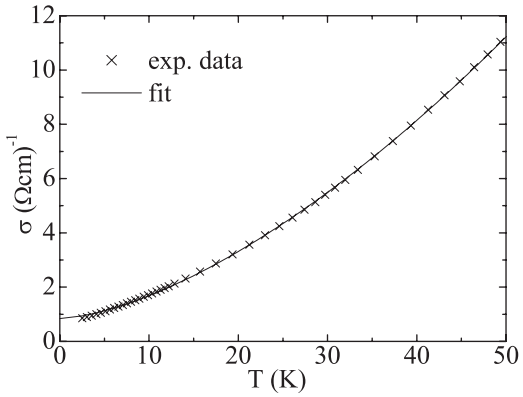

Figure 6. The conductivity $\sigma(T)$ for a ribbon with $R = 175$ between 2.5 and 50 K. The continuous curve corresponds to the fit $\sigma(T) = \sigma_0 + \sigma_1 T^{3/2} + \sigma_2 T^2$, with $\sigma_0 = 0.84$, $\sigma_1 = 0.025$ and $\sigma_2 = 0.0065$ (σ in $(\Omega\,\mathrm{cm})^{-1}$ and T in K).

figure 6 for an intermediate temperature range (3–50 K). We must include in the fit a constant σ_0 which was also mentioned in disordered systems analysis [25] and the significance of which is still unclear. Within the Anderson MI transition picture, this constant might come from a high temperature contribution of extended states lying beyond the mobility edge. The limit between the Thouless regime and the critical electron–phonon scattering regime is not clearly defined. Indeed, the exponent might become larger entering the electron–phonon range (around 3) if the sample stays in the Thouless regime or slower if it enters into the critical regime. Experimentally, the exponent is almost constant with temperature, around 1.5, which seems to indicate that highly resistive ribbons no longer follow the Thouless regime around 300 K.

Lastly, the very low temperature decrease below T_0^* was interpreted as the onset of a variable range hopping regime. The parameters extracted from the fit are quite unusual for the validity range of the theory [4] (very large localization lengths, $T > T_0$). Such a problem is also observed in some disordered insulators very close to the transition [29]. Note that there is no conductivity constant added for the Mott's law fit: the sample can truly be classified as an insulator. In any case, the transition temperature T_0^* and the Mott's temperature T_0 that could be extracted from the fits increase with R, as expected from the model.

4.2. Comparison with other experimental results

4.2.1. Disordered systems experiments. Our main emphasis here is the strong similarity between the $\sigma(T)$ behaviour in our insulating i-AlPdRe ribbons and in disordered systems. This was already pointed out for the crossing of the transition [7] and for insulating samples at very low temperature [4] ($T < 1$ K), and we have shown here it is also true in the higher temperature range 1–300 K. For disordered systems, one of the most thorough conductivity studies was performed in In–O disordered films [25]. These films have been measured and analysed extensively on both sides of the MI transition. The $\sigma(T, n)$ curves of this disorder system are barely distinguishable from the $\sigma(T, R)$ curves of i-AlPdRe ribbons. In In–O samples and close to the MI transition, the $\sigma(T, n)$ curves are roughly parallel to each other and linear at high enough temperature. Deeper in the insulating regime, the curves are no longer parallel but are characterized by power laws $AT^{3/2} + BT^3$ between 50 and 300 K, which is attributed to the Thouless regime. The first term comes from the electron–electron scattering contribution, and the second from the electron–phonon scattering. A constant σ_0 is

also introduced. At lower temperature, the authors also report a plateau-like conductivity, with a finite conductivity extrapolation at 0 K and a rapid further decrease of the conductivity at even lower temperatures described by Mott's law. In this system, the extracted Mott temperature T_0 stays above the maximum temperature of the Mott's law fit.

Other systems share many characteristics with i-AlPdRe ribbons, although the details can differ slightly from one system to an other. For example, the increase of the exponent α with the resistivity reported in table 1 is also obtained in bronze samples [30].

4.2.2. Other experiments on i-AlPdRe insulating samples. Most of the measurements on i-AlPdRe samples have focused on the low temperature range (below 20 K) and the whole temperature range up to 300 K is less often discussed.

Close to the MI transition and on the insulating side, the conductivity curves $\sigma(T)$ measured on different types of samples are all very similar. But the interpretations differ according to the authors. Very often, and contrary to what is proposed here, the low temperature negative concavity region (between T_1^* and T_2^*) is not analysed in terms of the critical regime but is attributed to Mott's VRH law [8, 9]. The main drawback of this interpretation is that it does not respect the symmetry across the transition. Namely, critical conductivity laws if present close to the MI transition on the metallic side must also be observed close to the transition on the insulating side. Moreover, if this negative range is due to VRH, how can we explain the further decrease of the conductivity observed at very low temperature when R is increased? Lastly, a constant was added to Mott's law in order to fit the data. Its physical meaning is still unexplained. In our view, the problem is the limited temperature range (not more than one decade) where conductivity data are fitted with Mott's law. This is indeed not broad enough to discriminate a Mott's law from a power law temperature dependence [15].

For more resistive samples (higher R), significant differences between $\sigma(T)$ curves of ribbons and ingots of same R are reported at low temperatures [31–33]. Comparison between the different samples then becomes difficult. We have suggested that these differences come from differences in chemical homogeneity [31]. Scanning electron microscope investigations have shown that ingots contain a large proportion of holes and suffer important chemical non-homogeneity. Our ribbons are instead not porous and more homogeneous [34], but careful chemical analysis reveals a small chemical gradient (around 0.5 at.%) in their thickness. If we assume a strong sensitivity of the low temperature conductivity to chemical composition, by similarity with doping in disordered insulators, the small gradient in the thickness of the ribbons may induce a different temperature dependence for the whole conductivity than the scattered and random chemical inhomogeneities of the ingots. Similar problems were also observed in disordered systems. For example, in Ni–Si amorphous samples made by different groups, the differences in $\sigma(T)$ curves were supposed to come from sample homogeneity or oxidation [35].

Magnetoconductivity data at low temperature of insulating i-AlPdRe samples are in agreement with what is found in disordered insulating systems [3, 36, 37]. Detailed analyses [33, 38, 39] based on disordered systems theories have been proposed. But it is difficult to validate or invalidate our interpretation from these studies since the magnetoconductivity problem is not fully solved even in conventional disordered systems. However, magnetoconductivity data of metallic i-AlPdRe samples are well described by weak localization theories ($R < 10$) [10]. It is found that τ_T between 40 mK and 4 K follows the law $\tau_T \propto T^p$ with $p \simeq 1.1$–1.5, which is in agreement with the values of p used in our interpretation of insulating $\sigma(T, R)$ curves.

In the temperature range 30–300 K, the power law equation (1) reported here was also mentioned by other authors [3, 5, 6]. They all obtain similar α values and an increase of α

from 1 to roughly 1.5 with R. This power law is sometimes interpreted as the signature of a quasicrystalline specific regime (see below).

4.3. Quasicrystalline specificity?

Specific quasicrystalline models have been proposed for the conductivity. From a phenomenological point of view, conductivity has been proposed [40] to arise from a hopping mechanism with a rate $\tau(T)$ between electron confining entities of typical size L_0. This can be also viewed as an interband scattering mechanism. This yields

$$\sigma(T) = e^2 N(E_F) \frac{L_0^2}{\tau(T)}, \tag{8}$$

where $1/\tau(T) = 1/\tau_{el} + 1/\tau_T$, τ_{el} being the elastic scattering time. Equation (8) gives an explanation for the unusual relation between the amount of structural defects and the conductivity value in highly resistive icosahedral alloys. Namely, the conductivity decreases when the structural quality is improved as shown in i-AlCuFe and i-AlPdMn [40]. Relation (8) is close to that of the Thouless regime, since the microscopic processes are similar. In the case where $N(E_F)$ is independent of composition and disorder, relation (8) would yield parallel $\sigma(T)$ for different defect levels, contrary to the Thouless regime. Indeed, this law was used in i-AlCuFe [40] and i-AlPdMn systems [41], in order to explain the parallelism of the curves from 100 K up to high temperatures.

Numerical and exact calculations on quasiperiodic systems have shown that electronic wavepackets spread anomalously [42, 43]. As in the critical regime discussed previously, it is equivalent to a length scale dependent diffusion coefficient $D = A{\tau_T}^{2\beta-1}$. Here β depends on the parameters of the system and the energy considered. Einstein's law gives the so-called generalized Drude law:

$$\sigma(T) \propto {\tau_T}^{2\beta-1}. \tag{9}$$

We point out that these two specific quasicrystalline models do not take into account interference effects due to disorder (chemical or structural) which will always be present in any actual sample. In fact, these models are valid [44] for length scales smaller than the elastic mean free path L_{el}, which is precisely the range where disordered systems models do not apply. The condition $L_T = L_{el}$ gives some crossover temperature T_{QC}, below which the sample should behave like in a disordered system, and above which it could follow QC laws. Such a temperature is unfortunately unknown. In i-AlCuFe ribbons, quantum interference effects in the weak localization regime seem to describe [11] the magnetic field and temperature dependence of conductivity up to $\simeq$100 K. Estimates of the elastic mean free path [44] give values as low as $\simeq$20 Å, which is of the order of the elementary clusters of the structure and which questions the existence of the quasicrystalline specific regime. For example, the density of states of highly resistive icosahedral samples is disordered like at least up to 100 meV in energy [44]. Above 300 K, other phenomena, like atomic vibrations around equilibrium positions (Debye–Waller mechanism), will play a leading role in the temperature increase of the conductivity [12, 45].

An alternative explanation to ours can be worked out within the theoretical quasicrystalline framework. We have to assume that T_{QC} lies in our measurement range, and that similarly [40] to i-AlCuFe, the higher the structural order the lower the conductivity. At high enough temperature ($T > T_{QC}$) the $\sigma(T, R)$ curves are parallel, following equation (8). At low temperature, all samples are disordered-like (long length scales) and the interpretation of section 4.1 remains valid. In the intermediate temperature, the more disordered ribbons (of lesser resistivity) become disordered-like, but the high resistive ribbons (more ordered) could

still be in the non-disordered QC regime: the power law dependence observed from 10 up to 100 K for ribbons around $R \simeq 100$ would then be attributed to QC laws like equation (9), as has been suggested by some authors [46, 47]. However, such a description relies on speculative assumptions in i-AlPdRe like the change of L_{el} with R and T_{QC} values below 300 K.

5. Summary

In conclusion, a coherent interpretation of the set of curves $\sigma(T, R)$ for i-AlPdRe ribbons with $T = 20$ mK–300 K and $R = 2$–200 is proposed. Insulating samples are especially discussed ($R = 16$–200). The strong similarities with disordered systems close to the Mott–Anderson MI transition is emphasized. The critical and the Thouless regimes, that are concepts developed for disordered systems, are the key ingredients of this interpretation. Our results agree with previous studies focusing on the analysis of metallic samples. No convincing evidence for a specific quasicrystalline insulating behaviour is found in the temperature range investigated. Icosahedral order is certainly essential in order to permit a strong localization in i-AlPdRe samples, but disordered-like quantum effects seem ultimately responsible for the strong variations of conductivity with temperature.

Acknowledgments

We wish to acknowledge J C Grieco for his help in preparing the samples and J P Brison for the conductivity measurements down to 10 mK.

References

[1] Pierce F S, Guo Q and Poon S J 1994 *Phys. Rev. Lett.* **73** 2220
[2] Akiyama H, Honda Y, Hashimoto T, Edagawa K and Takeuchi S 1993 *Japan. J. Appl. Phys.* **32** L1003
[3] Gignoux C, Berger C, Fourcaudot G, Grieco J C and Rakoto H 1997 *Eur. Phys. Lett.* **39** 171
[4] Delahaye J, Brison J P and Berger C 1998 *Phys. Rev. Lett.* **81** 4204
[5] Lin C R, Lin S T, Wang C R, Chou S L, Horng H E, Cheng J M, Yao Y D and Lai S C 1997 *J. Phys.: Condens. Matter* **9** 1509
[6] Honda Y, Edagawa K, Yoshioka A, Hashimoto T and Takeuchi S 1994 *Japan. J. Appl. Phys.* **33** 4929
[7] Delahaye J and Berger C 2001 *Phys. Rev.* B **64** 094203
[8] Wang C R and Lin S T 1994 *J. Phys. Soc. Japan* **66** 3988
[9] Rosenbaum R, Haberkern R, Haussler P, Palm E, Murphy T, Hannahs S and Brandt B 2000 *J. Phys.: Condens. Matter* **12** 9735
[10] Rodmar M, Ahlgren M, Oberschmidt D, Gignoux C, Delahaye J, Berger C, Poon S J and Rapp O 2000 *Phys. Rev.* B **61** 3936
[11] Linqvist P, Lanco P, Berger C, Jansen A G M and Cyrot-Lackmann F 1995 *Phys. Rev.* B **51** 4796
[12] Klein T 1992 *PhD Thesis* Grenoble University
[13] Delahaye J, Berger C, Gignoux C, Fourcaudot G and Grieco J C 2003 at press
[14] Poon S J, Zavaliche F and Beeli C 1999 *Quasicrystals* (*Materials Research Society Symp. Proc.* vol 553) ed J M Dubois, P A Thiel, A P Tsai and K Urban (Pittsburgh, PA: Materials Research Society) p 365
[15] Delahaye J, Brison J P, Berger C and Fourcaudot G 2000 *Mater. Sci. Eng.* A **294–296** 580
[16] Imry Y 1980 *Phys. Rev. Lett.* **44** 469
[17] Imry Y 1981 *J. Appl. Phys.* **52** 1817
[18] Imry Y and Ovadyahu Z 1982 *J. Phys. C: Solid State Phys.* **15** L327
[19] Abrahams E, Anderson P W, Licciardello D C and Ramakrishnan T V 1979 *Phys. Rev. Lett.* **42** 673
[20] Mott N F 1968 *J. Non-Cryst. Solids* **1** 1
[21] Mott N F 1990 *Metal–Insulator Transitions* 2nd edn (London: Taylor and Francis)
[22] Ladieu F and Sanquer M 1996 *Ann. Phys. Fr.* **21** 267
[23] Thouless D J 1977 *Phys. Rev. Lett.* **39** 1167

[24] Thouless D J 1978 *The Metal Non-Metal Transition in Disordered Systems* ed L R Friedman and D P Tunstall (Warrendale, PA: MRS) p 61
[25] Ovadyahu Z 1986 *J. Phys. C: Solid State Phys.* **19** 5187
[26] Schmid A 1973 *Z. Phys.* **259** 421
[27] Altshuler B L and Aronov A G 1985 *Electron Electron Interactions in Disordered Systems* ed A L Efros and M Pollak (Amsterdam: North-Holland) p 1
[28] Pierce F S, Poon S J and Guo Q 1993 *Science* **261** 737
[29] Castner T G and Shafarman W N 1999 *Phys. Rev.* B **60** 14182
[30] Raychaudhuri A K 1991 *Phys. Rev.* B **44** 8572
[31] Rodmar M, Oberschmidt D, Ahlgren M, Gignoux C, Delahaye J, Berger C, Poon S J and Rapp O 1999 *J. Non-Cryst. Solids* **250–252** 883
[32] Rodmar M, Zavaliche F, Poon S J and Rapp O 1999 *Phys. Rev.* B **60** 10807
[33] Srinivas V, Rodmar M, Konig R, Poon S J and Rapp O 2002 *Phys. Rev.* B **65** 094206
[34] Delahaye J, Gignoux C, Schaub T, Berger C, Grenet T, Sulpice A, Préjean J J and Lasjaunias J C 1999 *J. Non-Cryst. Solids* **250–252** 878
[35] Möbius A, Frenzel C, Thielsch R, Rosenbaum R, Adkins C J, Schreiber M, Bauer H D, Grötzchel R, Hoffman V, Krieg T, Matz N, Vinzelberg H and Witcomb M 1999 *Phys. Rev.* B **60** 14209
[36] Poon S J, Pierce F S and Guo Q 1995 *Phys. Rev.* B **51** 2777
[37] Wang C R, Kuan H S, Lin S T and Chen Y Y 1998 *J. Phys. Soc. Japan* **67** 2383
[38] Srinivas V, Rodmar M, Poon S J and Rapp O 2001 *Phys. Rev.* B **63** 172202
[39] Su T I, Wang C R, Lin S T and Rosenbaum R 2002 *Phys. Rev.* B **66** 054438
[40] Mayou D, Berger C, Cyrot-Lackmann F, Klein T and Lanco P 1993 *Phys. Rev. Lett.* **70** 3915
[41] Préjean J J, Berger C, Sulpice A and Calvayrac Y 2002 *Phys. Rev.* B **65** 14203(R)
[42] Mayon D 2000 *Quasicrystals, Current Topics* ed E Belin-Ferré, C Berger, M Quiquandon and A Sadoc (Singapore: World Scientific) p 412 and reference therein
[43] Fujiwara T 1999 *Physical Properties of Quasicrystals* (*Springer Series in Solid-State Sciences* vol 126) ed Z M Stadnink (Berlin: Springer) p 169 and references therein
[44] Delahaye J, Schaub T, Berger C and Calvayrac Y 2003 *Phys. Rev.* B **67** 214201
[45] Haberkern R, Khedhri K, Madel C and Häussler P 2000 *Mater. Sci. Eng.* A **294–296** 475
[46] Roche S and Fujiwara T 1998 *Phys. Rev.* B **58** 11338
[47] Bellissard J 2000 *Mater. Sci. Eng.* A **294–296** 450